Electronic Supplementary Information (ESI)

Two Fully Conjugated Covalent Organic Frameworks as Anode Materials for Lithium Ion Batteries

Linyi Bai,[a] Qiang Gao,[a] Yanli Zhao*[,a,b]

[a]Division of Chemistry and Biological Chemistry, School of Physical and Mathematical Sciences, Nanyang Technological University, 21 Nanyang Link, Singapore 637371

[b]School of Materials Science and Engineering, Nanyang Technological University, 50 Nanyang Avenue, Singapore 639798

Email: zhaoyanli@ntu.edu.sg

1. Materials and instruments

All reagents and chemicals were purchased commercially from Sigma-Aldrich and used without further purifications unless otherwise stated.

1.1 Powder XRD and CV measurements

Powder XRD studies were performed on a SHIMADZU XRD-6000 Labx diffractometer using Cu-Ka radiation at 40 kV and 300 mA with a scanning rate of 0.02^{o} s^{-1} (2θ) at room temperature. Electrochemical cyclic voltammetry (CV) was performed using a Grammy electrochemical workstation in a 0.1 mol/L tetrabutylammoniumhexafluorophosphate (Bu_4NPF_6) dichloromethane (DCM) solution with a scan speed at 0.1 V/s. Pt wire and Ag/AgCl were used as the counter and reference electrodes, respectively. The concentration of samples was adjusted as 1×10^{-4} M in chromatographic pure DCM solution for the CV measurements.

1.2 STM measurements

The LT-STM/STS experiments were performed in a multi-chamber UHV system housing an Omicron LT-STM. STM imaging was carried out at 77 K in constant current mode with a chemically etched tungsten tip. Imaging conditions: V_{bias} = 600 mV, It = 500 pA.

1.3 Gas adsorption

Low-pressure gas sorption measurements were performed by using Quantachrome Instruments Autosorb-iQ (Boynton Beach, Florida USA) with the extra-high pure gases. Before the measurements, an activation process for the as-synthesized COFs was performed, in which the COFs were rinsed with DMF for three times, followed by solvent exchange with CH_2Cl_2 for six times. CH_2Cl_2 was further removed with supercritical liquid CO_2 in a Tousimis Samdri PVT-30 critical point dried by the following procedures. The wet sample was placed inside the dryer and CH_2Cl_2 was exchanged with liquid CO_2 over a period of 20 minutes, during which time the liquid CO_2 was vented under a positive pressure. The venting rate of liquid CO_2 was kept below the rate of filling so as to maintain a full chamber. After 20 minutes of venting and soaking with liquid CO_2, the temperature was raised to 40 °C. The chamber was held above the critical point with the pressure around 1300 psi for 1 hour, at which point the chamber was slowly vented over 12 hours. This activation method was recently adopted to activate COFs, which is different from the approach used in our previous

reports.[S1,S2] By using the present method, the gas sorption property of these two COFs including N_2 isotherms and gas selective adsorption was improved.

1.4 Tapped density measurements

Tapped density (g/mL) of N-COFs was calculated using the formula of m/V_f, where m is the weight of fine powder and V_f is the final tapped volume. During this measurement, the weighted powder was put in a graduated measuring cylinder followed by a mechanically tapping. Then, a tapping volume (V_f) was obtained. Subsequently, a calculation of m/V_f was carried out to give a tapped density of the powder sample.

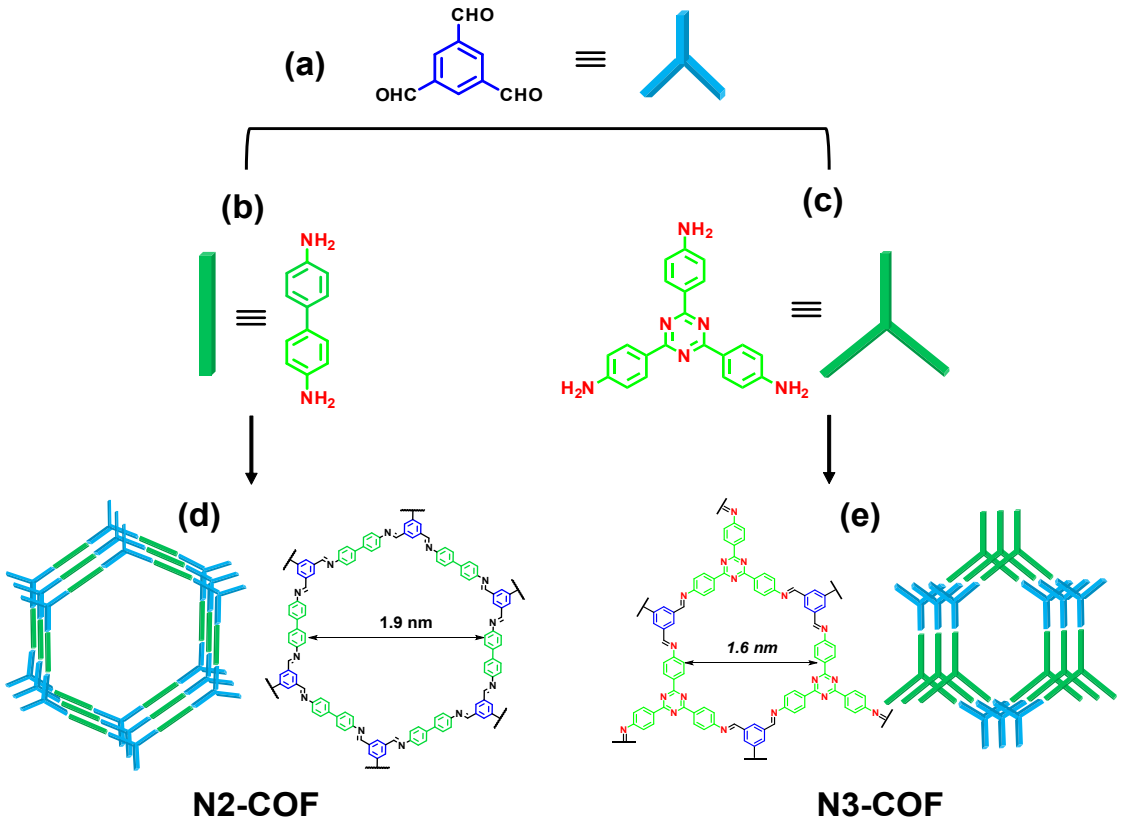

Figure S1. Schematic illustration of COF formations by a condensation of (a) 1,3,5-triformylbenzene and two amino derivatives, (b) 4,4'-biphenyldiamine and (c) 2,4,6-tris(4-aminophenyl)-s-triazine, to give two polyimine-based COFs, i.e., (d) N2-COF and (e) N3-COF. Controlled self-assembly affords the COF products with porous structures having tunable pore width and layered stacking. Green color represents the amino derivatives and blue color stands for the 1,3,5-triformylbenzene unit.

2. Experimental details

2.1 Synthesis of N2-COF

Anhydrous 1,4-dioxane, anhydrous mesitylene, anhydrous THF and 4,4'-biphenyldiamine were purchased from Sigma-Aldrich. 1,3,5-Triformylbenzene was synthesized according to the reported procedure.[S1] 4,4'-Biphenyldiamine (83 mg, 0.3 mmol) and 1,3,5-triformylbenzene (48 mg, 0.2 mmol) were weighed into a 25 mL Schlenk storage tube (SynthwareTM, OD28 x L120mm, high vaccum valve size 0-8mm, with PTFE o-ring and wiper), dissolved in mixed solvent (3 mL, 1,4-dioxane:mesitylene = 1:1) and sonicated for 10 min. After that, aqueous HOAc (0.3 mL, 6 mol/L) was added to the mixture. Each tube was degassed by three freeze-pump-thaw cycles. Finally, each tube was sealed off, heated at 120 ºC in an oven at the same time, and left undisturbed for 0-72 h. The precipitates were isolated by centrifugation, washed with anhydrous THF for 3 times, and dried at 120 ºC under vacuum for 24 h, to give a yellow powder with 75-90 % isolation yields. The tapped density of N2-COF was measured to be 0.17 g/mL.

2.2 Synthesis of N3-COF

2,4,6-Tris(4-aminophenyl)-1,3,5-triazine was synthesized according to the reported procedures.[S2] The ^{1}H NMR and ^{13}C NMR spectra matched well with those reported ones. Then, 2,4,6-tris(4-aminophenyl)-1,3,5-triazine (70 mg, 0.2 mmol) and 1,3,5-triformylbenzene (48 mg, 0.2 mmol) were placed in a 25 mL Schlenk storage tube, which were dissolved in a mixture solvent (10 mL, 1,4-dioxane : mesitylene = 10:1, v:v) and sonicated for 10 min. After that, aqueous HOAc (0.75 mL, 6M) was added, and the mixture was degassed by three freeze-pump-thaw cycles. Finally, the tube was sealed, heated at 120 ^{o}C in an oven, and left undisturbed for 72 h. The precipitate was collected through centrifugation, which was washed with anhydrous THF for 3 times, and then dried at 150 °C under vacuum for 24 h. A yellow powder was obtained in 90% isolation yield. The tapped density of N3-COF was measured to be 0.22 g/mL.

2.3 Theoretical calculations

Density functional theory calculations were performed with the Gaussian 09 program using the B3LYP functional.[S3] All-electron double-ξ valence basis sets with polarization functions 6-31G* were used for all atoms.[S3] Geometry optimizations were performed with full

relaxation of all atoms in gas phase without solvent effects.

3. Structural modeling

3.1 Simulated CIF data of N2-COF and N3-COF could be found from our previous reports.[S1,S2]

3.2 Predicted stacking mode and practical powder XRD pattern.

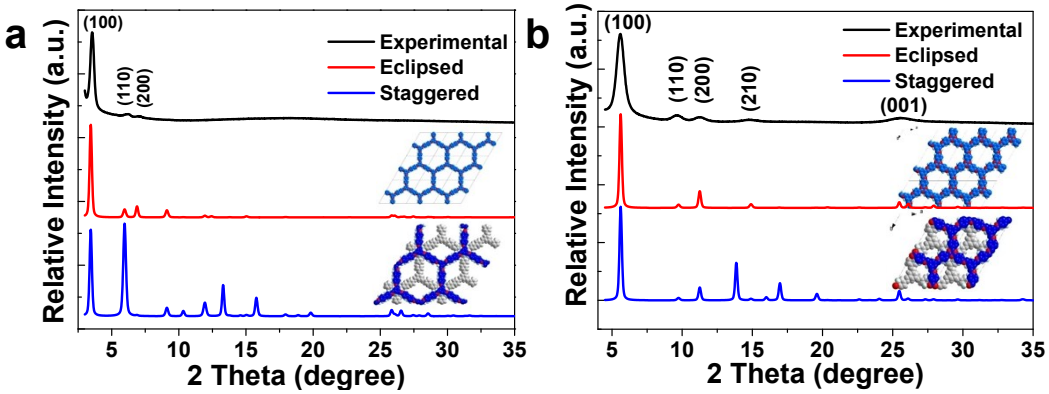

Figure S2. Theoretical calculation and practical powder XRD patterns of (a) N2-COF and (b) N3-COF: experimental powder XRD pattern (black curve) and simulated patterns of eclipsed (red) and staggered (blue) structures. Inset figures are simulated crystal lattice of the unit cells calculated in an eclipsed (upper) and staggered structure (down).

4. Physical properties

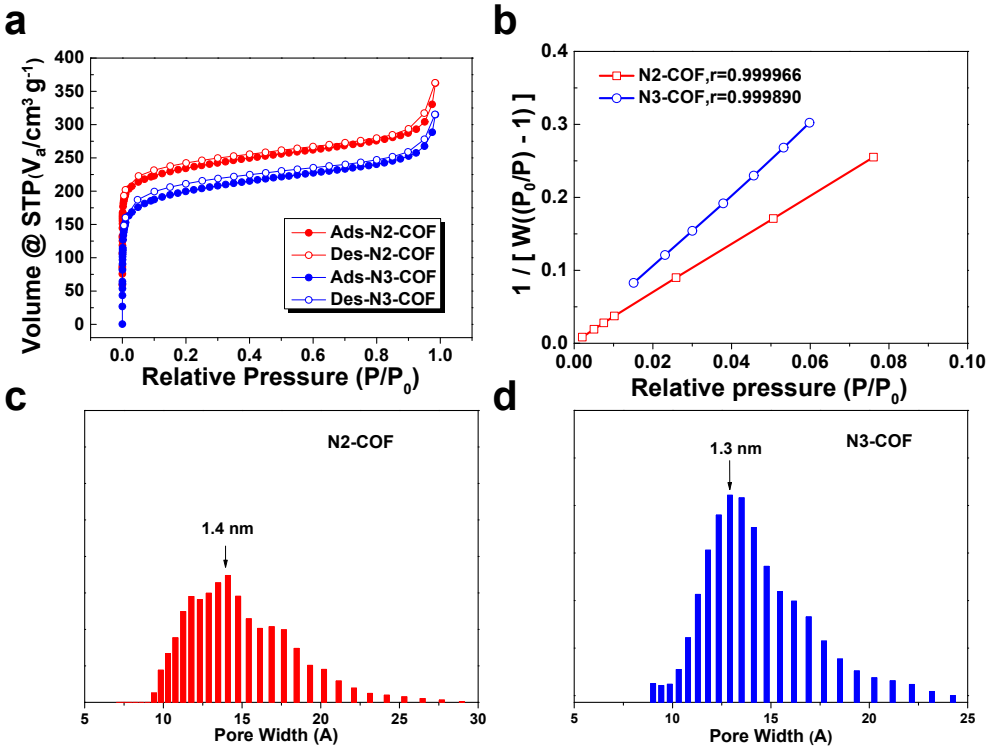

Figure S3. (a,b) N_2 isothermal adsorption curves and BET of N-COFs. (c,d) Pore-size

distribution plots of two N-COFs calculated from experimental N_2 adsorption isotherms using the nonlocal density functional theory (NLDFT): N2-COF (red curve) and N3-COF (blue curve).

5. T-plot method

Table S1 T-plot method for microporous and mesoporous measurements.

	N2-COF	**N3-COF**
[a]Total pore volume (cc/g)	0.622	0.561
[b]Micropore volume (cc/g)	0.387	0.313
[c]Mesopore volume (cc/g)	0.235	0.248
[b]Micropore area (m^2/g)	1304.7	942.0
[b]External surface area (m^2/g)	191.3	159.0

Determined by N_2 adsorption/desorption isotherms at 77K: [a] calculated by the point of the highest adsorption; [b] determined by the t-plot method, where the contribution points are from 0.35-0.5 in P/P_0; [c] obtained by the difference between the total pore volume and micropore volume.

6. Lithium ion battery fabrication

Standard CR2032-type coin cells were assembled in an argon-filled glovebox (Mbraun, Unilab, Germany) with the as-fabricated N-COFs as the working electrode (0.5cm × 0.5 cm, 0.25 cm^2). The average loading of N-COFs in each battery is ~3.1 mg, and the anode was made without adding any binders. For lithium ion battery fabrication, the metallic lithium foil served as the counter-electrode, it was separated from the working electrode by a Celgard 2500 polymeric separator. The electrolyte was composed of a solution of 1 M $LiPF_6$ in ethylene carbonate (EC) / dimethyl carbonate (DMC) / diethyl carbonate (DEC) (1:1:1 by volume). The cells were assembled in an argon-filled glovebox with the concentrations of moisture and oxygen at less than 1 ppm. The CV measurements were carried out using a Parstat-2273 electro-chemical potentiostat at a scanning rate of 0.2 mV/s. Galvanostatic charge−discharge cycles were tested by Neware battery tester at different current densities at room temperature. There was a slight shift between the first cycle and the cycles after the

third cycle in the CV measurements, which may be caused by the initial unstable state of electrolyte and electrode materials. During the charge-discharge progress, the solid electrolyte interphase (SEI) was formed on the surface of electrodes using N-COFs, which predominantly contained lithium ethylene dicarbonate, lithium methyl carbonate and LiF.[S4]

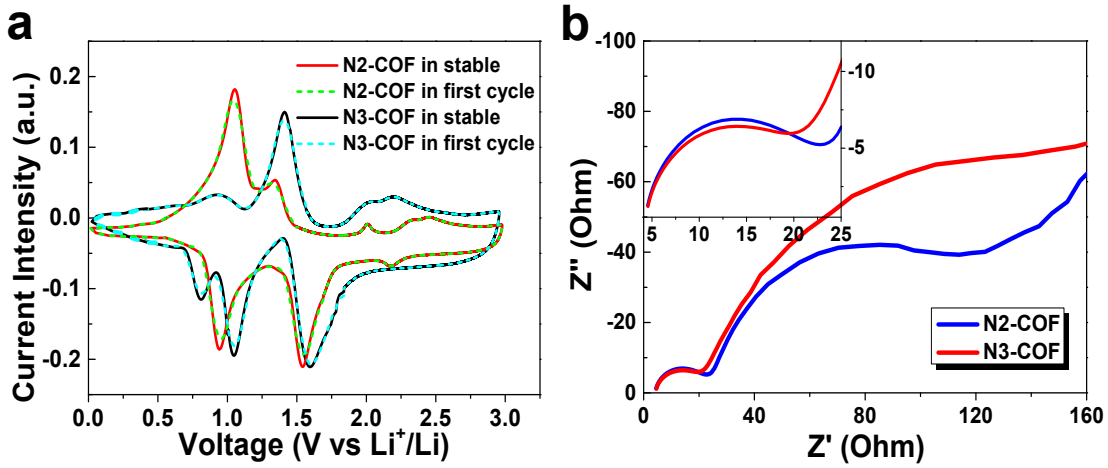

Figure S4. Electrochemical performance of LIBs fabricated based on N2-COF and N3-COF anodes: (a) CV curves of two N-COFs used as anodes in LIBs, where the dash curves showed the electrochemical performance of N-COFs in the first cycle and the solid curves presented the electrochemical performance of N-COFs after the third cycle; (b) Nyquist plots of two N-COFs electrodes: N2-COF (blue curve) and N3-COF (red curve). Inset shows alternating current impedance plots at the full-charged state after the first cycle. The resistance was simulated using an equivalent circuit of RS(Q(R_{ct}ZW)), where RS is the ohmic resistance of solution and electrode, R_{ct} is the charge transfer resistance, Q is the double layer capacitance, and ZW is the Warburg impedance.

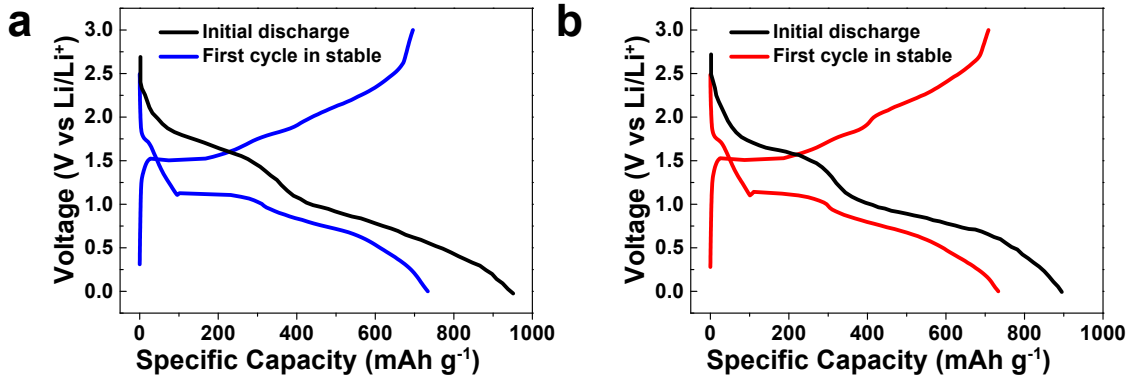

Figure S5. Comparison of initial discharge (the first cycle) and stable first discharge (the

second cycle) of two N-COFs: (a) N2-COF and (b) N3-COF.

7. Electrode reactions in the charge-discharge process

According to the structure of two N-COFs, their electrode reactions occurred in the charge-discharge progress are shown in Figure S6, where N2-COF undergoes a two-electron redox reaction and N3-COF follows a three-electron redox reaction during the lithiation and delithiation. In comparison with previous reports,[S5] the electrode potential of the Schiff base generally locates in the range of 0.8-2.0 eV, which matches well with our experiment results.

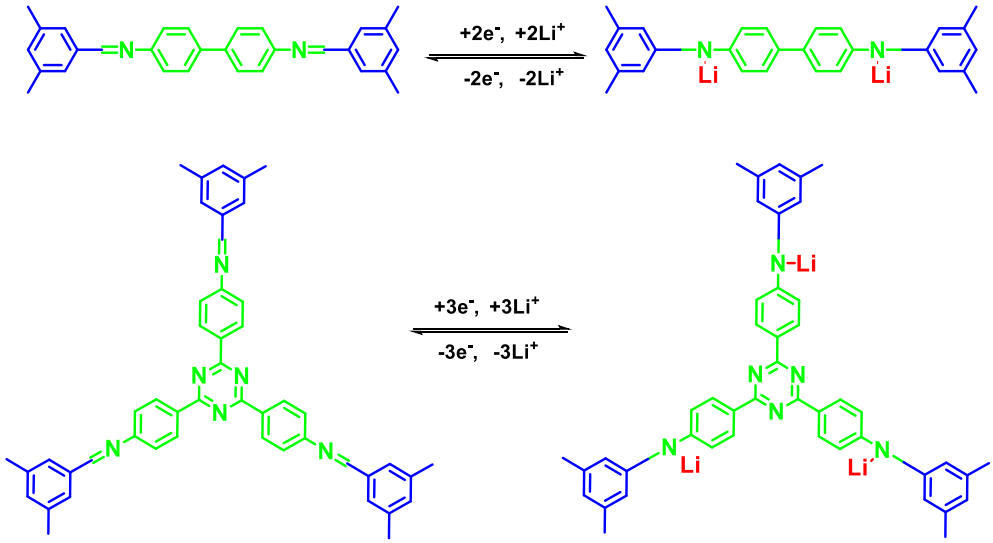

Figure S6. Electrochemical reactions of a unit of N-COFs during the charge-discharge progress.

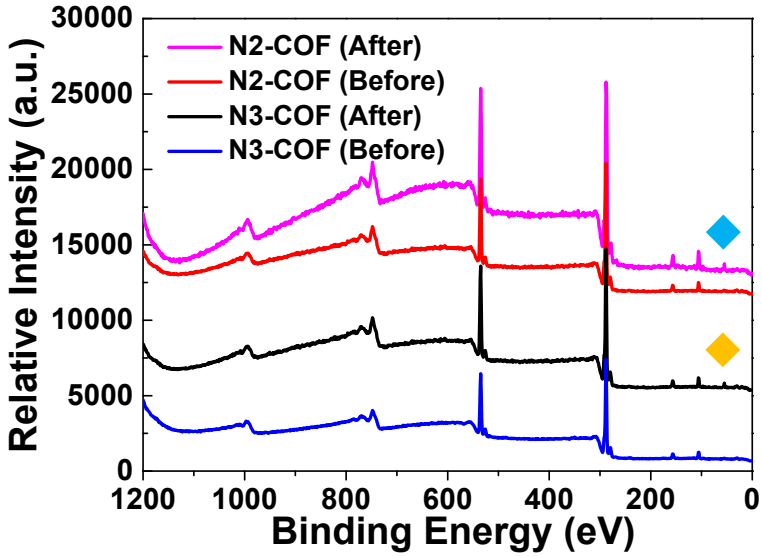

Figure S7. XPS spectra of the N-COF electrodes showing the difference before and after the charge-discharge progress.

8. Charge limited current mobility measurements

To characterize the electronical conductivity, the charge limited current mobility measurement was performed, where the device was fabricated with a configuration of ITO / PEDOT:PSS / N-COF / MoO_3 / Al. The individual active film is of typical organic solar cell device area (0.25 cm^2). The J–V characteristics of the hole-only devices are shown in Figure S8.

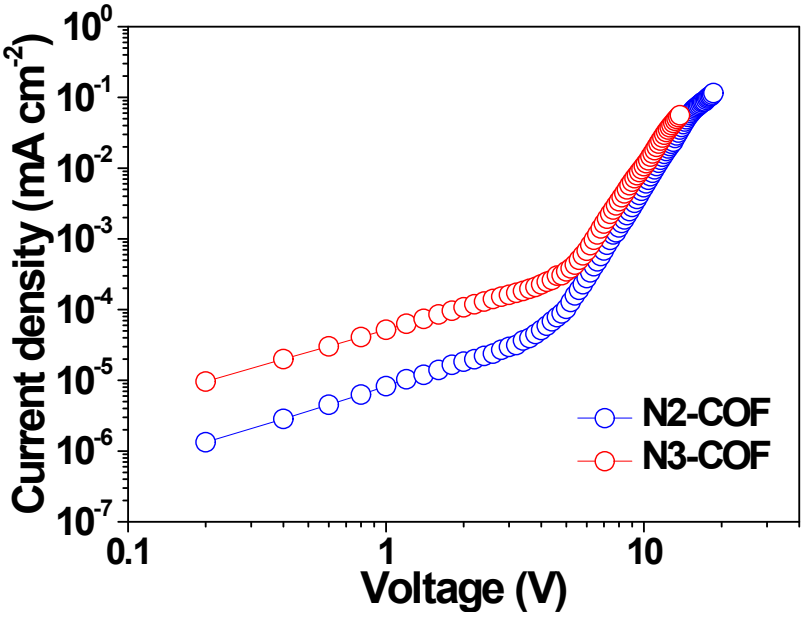

Figure S8. Current density–voltage characteristics of the hole-only devices based on thin films of N2-COF and N3-COF with the configuration of ITO / PEDOT:PSS / N-COF / MoO_3 / Al after thermal annealing at 110 ºC.

9. References

(S1) Q. Gao, L. Bai, Y. Zeng, P. Wang, X. Zhang, R. Zou and Y. Zhao, *Chem. Eur. J.*, 2015, **21**, 16818-16822.

(S2) Q. Gao, L. Bai, X. Zhang, P. Wang, P. Li, Y. Zeng, R. Zou and Y. Zhao, *Chin. J. Chem.*, 2015, **33**, 90-94.

(S3) M. J. Frisch, G. W. Trucks, H. B. Schlegel, G. E. Scuseria, M. A. Robb, J. R. Cheeseman, G. Scalmani, V. Barone, B. Mennucci, G. A. Petersson, H. Nakatsuji, M. Caricato, X. Li, H. P. Hratchian, A. F. Izmaylov, J. Bloino, G. Zheng, J. L. Sonnenberg, M. Hada, M. Ehara, K. Toyota, R. Fukuda, J. Hasegawa, M. Ishida, T. Nakajima, Y. Honda, O. Kitao, H. Nakai, T.

Vreven, J. A., Jr. Montgomery, J. E. Peralta, F. Ogliaro, M. Bearpark, J. J. Heyd, E. Brothers, K. N. Kudin, V. N. Staroverov, R. Kobayashi, J. Normand, K. Raghavachari, A. Rendell, J. C. Burant, S. S. Iyengar, J. Tomasi, M. Cossi, N. Rega, J. M. Millam, M. Klene, J. E. Knox, J. B. Cross, V. Bakken, C. Adamo, J. Jaramillo, R. Gomperts, R. E. Stratmann, O. Yazyev, A. J. Austin, R. Cammi, C. Pomelli, J. W. Ochterski, R. L. Martin, K. Morokuma, V. G. Zakrzewski, G. A. Voth, P. Salvador, J. J. Dannenberg, S. Dapprich, A. D. Daniels, Ö. Farkas, J. B. Foresman, J. V. Ortiz, J. Cioslowski and D. J. Fox, Gaussian 09, Revision A.02, Gaussian, Inc., Wallingford CT, 2009.

(S4) (a) E. Peled, C. Menachem, D. Bar-Tow and A. Melman, *J. Electrochem. Soc.*, 1996, **143**, L4-L7; (b) D. Aurbach, B. Markovsky, A. Shechter, Y. Ein-Eli and H. Cohen, *J. Electrochem. Soc.*, 1996, **143**, 3809-3820.

(S5) (a) E. Castillo-Martínez, J. Carretero-González and M. Armand, *Angew. Chem. Int. Ed.*, 2014, **126**, 5445–5449; (b) Y. Sun, Y. Sun, Q. Pan, G. Li, B. Han, D. Zeng, Y. Zhang and H. Cheng, *Chem. Commun.,* 2016, **52**, 3000-3002.